Inverse Green Element Solutions of Heat Conduction Using the Time-Dependent and Logarithmic Fundamental Solutions

Akpofure E. Taigbenu[1]

Abstract: The solutions to inverse heat conduction problems (IHCPs) are provided in this paper by the Green element method (GEM), incorporating the logarithmic fundamental solution of the Laplace operator (Formulation 1) and the time-dependent fundamental solution of the diffusion differential operator (Formulation 2). The IHCPs addressed relate to transient problems of the recovery of the temperature, heat flux and heat source in 2-D homogeneous domains. For each formulation, the global coefficient matrix is over-determined and ill-conditioned, requiring a solution strategy that involves the least square method with matrix decomposition by the singular value decomposition (SVD) method, and regularization by the Tikhonov regularization method. Comparisons of the two formulations are made using five numerical examples of transient IHCPs. Using the same spatial and temporal discretizations, the GEM with the logarithmic fundamental solution is generally more superior in accuracy and computational speed than the formulation with the time-dependent fundamental solution.

Keywords: Inverse heat conduction problems, Green element method, time dependent fundamental solution, logarithmic fundamental solution, singular value decomposition, Tikhonov regularization.

1   Introduction

The considerable interest that continues to attend the solution of inverse heat conduction problems (IHCPs) is due to their many practical applications in the fields of Engineering and the Sciences where heat, mass and energy transport processes occur and, from a computational perspective, the numerical intrigues and challenges that arise when solving these problems. The classes of IHCPs range from the recovery of temperature and heat flux [Cialkowski and Grysa (2010); Reinhardt et

---

[1] School of Civil and Environmental Engineering, University of the Witwatersrand. P. Bag 3, Johannesburg, WITS 2050. South Africa. E-mail: akpofure.taigbenu@wits.ac.za

al. (2007); Sladek et al. (2006)] to the estimation of flow and medium parameters [Char et al. (2008); Yang (1998); Sawaf et al. (1995)] to the recovery of the spatial and temporal distributions of heat sources/sinks [Wei and Wang (2012); Mierzwiczak and Kolodziej (2010); Yan et al. (2008)] to the recovery of initial data distributions [Pereverzyev et al. (2005); Masood et al. (2002)], and to the recovery of the geometric profiles of boundary and medium features [Yang et al. (2009); Mera et al. (2004)]. Two classes of IHCPs addressed in this paper are the recovery of boundary temperature and heat flux and that of the temporal distribution of heat sources/sinks. It is widely known that inverse problems are ill-posed so that the matrices resulting from solving them are usually ill-conditioned, in contrast to direct solution methods which produce well conditioned matrices. The degree of ill-conditioning of the inverse problem depends on the spatial and temporal distribution of the available measurements of temperature and as well as the boundary and initial data.

The performances of two formulations of the Green element method (GEM) are examined for these two classes of IHCPs. The GEM is a numerical technique whose theory is predicated on the singular integral theory of the boundary element method (BEM) but whose implementation is done in an element-by-element fashion so that the generated coefficient matrix is banded and amenable to efficient matrix solvers [Taigbenu (1999)]. In the first GEM formulation, the differential equation is treated as a Poisson equation to which the logarithmic fundamental solution of the Laplace operator is used and the temporal part of the equation is approximated by finite differencing in time [Taigbenu (1999; 2012)], while the second formulation uses the time-dependent fundamental solution of the heat equation. For both formulations, the internal normal fluxes are approximated by a second-order polynomial relationship in terms of the temperature [Taigbenu (2012)], and the resulting overdetermined matrices are decomposed by the singular value decomposition (SVD) method and solved by the least square method. The challenge posed by the ill-conditioned nature of the matrices is resolved by the Tikhonov regularization technique. Five numerical examples, of which two address the first class of problems and the other three the second class of IHCPs, are solved by the two GEM formulations. The GEM with the logarithmic fundamental solution generally achieves higher accuracy using about 3% of the computing time of the formulation with the time-dependent fundamental solution.

2 Governing Equation

The initial-boundary value problem that is addressed in this paper is governed by the differential equation

$$K\nabla^2 T = \rho c \frac{\partial T}{\partial t} + Q(t) \tag{1}$$

where ∇^2 is the 2-D Laplacian operator in the spatial variables x and y, t is the time dimension, T is the temperature, K is the thermal conductivity, ρ is the density, c is the specific heat capacity, and Q represents heat sources and sinks whose strengths have only temporal variation but are not known. The initial data of the temperature are specified everywhere in the domain Ω at time t_0,

$$T(x, y, t_0) = T_0(x, y) \tag{2a}$$

while Dirichlet, Neumann, and Cauchy-type conditions are specified on boundary segments Γ_1, Γ_2 and Γ_3. That is:

$$T(x, y, t) = T_1 \quad \text{on} \quad \Gamma_1 \tag{2b}$$

$$-K\nabla T \cdot \mathbf{n} = q_2 \quad \text{on} \quad \Gamma_2 \tag{2c}$$

$$\gamma_1 T + \gamma_2 K\nabla T \cdot \mathbf{n} = g_3 \quad \text{on} \quad \Gamma_3 \tag{2d}$$

where $\mathbf{n}$ is the unit outward pointing normal on the boundary, and γ_1 and γ_2 are known constants. The domain Ω with the boundary $\Gamma = \Gamma_1 \cup \Gamma_2 \cup \Gamma_3 \cup \Gamma_4$ is shown in Fig. 1, and neither the temperature T nor heat flux q is specified on Γ_4. For both types of IHCPs, temperature measurements are available at P internal points (x_m, y_m) in the domain and denoted as $T_m = T(x_m, y_m, t)$. In practice these measurements may have errors which can be described by the relationship

$$\tilde{T}_m = T_m[1 + \sigma \times RN(m)] \tag{3}$$

where σ is the error magnitude and $RN \in [-1, 1]$ are random numbers.

3 Green element formulations

3.1 Formulation 1

This formulation of GEM, referred to as Formulation 1, uses the logarithmic fundamental solution in its integral equation. It had earlier been presented in Taigbenu (2015) and for that reason it is only succinctly described in this paper. It treats
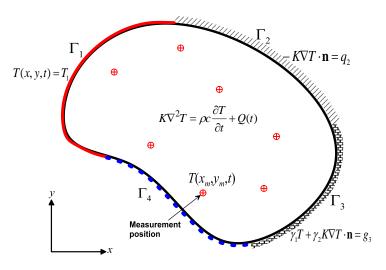
Figure 1: Domain and problem statement representation

Eq. 1 as a Poisson equation to which Green's theorem is applied, resulting in the singular integral equation that arises in boundary element formulations

$$K \left(\int_{\Gamma} T G^* \, ds - \lambda T_i \right) + \int_{\Gamma} G q \, ds + \iint_{\Omega} G \left[\kappa \frac{\partial T}{\partial t} + Q \right] dA = 0 \tag{4}$$

where $\kappa = \rho c$, $G = \ln(r - r_i)$ is the fundamental solution of the Laplace differential operator, $q = -K \nabla T \cdot \mathbf{n}$ is the normal heat flux, the subscript i represents the collocation point $r_i = (x_i, y_i)$ and λ is the nodal angle at r_i. The implementation of the integral Eq. 4 does not follow the classical approach in boundary element circles but employs the limiting case of the domain decomposition technique of element arrangement that is similar to finite elements [Popov (2007); Taigbenu (1999)]. The unknown quantities T and q are interpolated over the elements, that is $T \approx \phi_j T_j$ (ϕ_j are the spatial interpolation functions which, in this paper, are chosen to be linear). Introducing the interpolation relationship into Eq. 4 gives the elemental equations

$$R_{ij} T_j + L_{ij} q_j + W_{ij} \frac{dT_j}{dt} + F_i Q = 0 \tag{5}$$

where

$$R_{ij} = K \left(\int\limits_{\Gamma^e} \varphi_j G_i^* \, ds - \delta_{ij} \lambda \right), \quad L_{ij} = \int\limits_{\Gamma^e} \varphi_j G_i ds,$$

$$W_{ij} = \kappa \iint\limits_{\Omega^e} G_i \varphi_j \, dA, \quad F_i = \iint\limits_{\Omega^e} G_i \, dA \tag{6}$$

where Ω^e and Γ^e are the domain and boundary of an element e. The approach presented in Taigbenu (2012) is used to approximate the normal flux q at inter-element boundaries in terms of T which is expressed as a quadratic polynomial of the spatial variables. With this approximation, T and q are computed on the boundary of the computational domain and T within the domain. The temporal derivative term is approximated by a finite difference expression: $dT/dt \approx [T^{(2)} - T^{(1)}]/\Delta t$ evaluated at $t = t_1 + \beta \Delta t$, where $0 \leq \beta \leq 1$, is the difference weighting factor, and Δt is the time step between the current time t_2 and the previous one t_1. With this difference approximation, Eq. 5 becomes

$$\left(\beta R_{ij} + \frac{W_{ij}}{\Delta t} \right) T_j^2 + \beta L_{ij} q_j^2 + \beta F_i Q^2 = \left(\omega R_{ij} + \frac{W_{ij}}{\Delta t} \right) T_j^1 + \omega L_{ij} q_j^1 + \omega F_i Q^1 \tag{7}$$

where $\omega = \beta - 1$ and the superscripts represent the times at which the quantities are evaluated. The initial and boundary data and available internal temperature measurements are incorporated into Eq. 7 to give the matrix equation

$$\mathbf{Ap} = \mathbf{b} \tag{8}$$

Where

$$\mathbf{A} = \begin{bmatrix} \beta R_{ij} + W_{ij}/\Delta t \\ \beta B_{ij} \\ \beta F_i \end{bmatrix} \quad \text{and} \quad \mathbf{p} = \left\{ \begin{array}{c} T_j^2 \\ q_j^2 \\ Q^2 \end{array} \right\} \tag{9}$$

The vector $\mathbf{p}$ is an $N \times 1$ vector of unknowns at t_2 (T and/or q at external nodes, T at internal nodes and the heat source strength, Q). The right side $\mathbf{b}$ of Eq. 8 comprises the initial data and the specified boundary and observed data at interior points. The matrix $\mathbf{A}$ is an $M \times N$ matrix, where M is the number of nodes in the computational domain (which equals the number of discrete equations generated by the GEM formulation) and $M \geq N$.

3.2   Formulation 2

The integral representation of Formulation 2 arises from applying Green's theorem to Eq. 1, and integrating in time between t_0 and any time t to give the singular integral equation which is the same as that obtained in BEM [Brebbia et al. (1984)]

$$
\begin{aligned}
2\lambda T_i + \int_{t_0}^{t}\int_{\Gamma}[DT(r,\tau)G^*(r,r_i,t,\tau) + G(r,r_i,t,\tau)q(r,\tau)/\kappa]\,dsd\tau - \\
\iint_{\Omega}G(r,r_i,t,0)T(r,0)\,dA + \frac{1}{\kappa}\int_{t_0}^{t}Q(\tau)\iint_{\Omega}G(r,r_i,t,\tau)\,dAd\tau = 0
\end{aligned}
\tag{10}
$$

where

$$
G(r,r_i,t,\tau) = \frac{H(t-\tau)}{D(t-\tau)}\exp-\left[\frac{(r-r_i)}{4D(t-\tau)}\right]
\tag{11}
$$

is the fundamental solution of $D\nabla^2 G + \partial G/\partial t = -\delta(r-r_i)\delta(t-\tau)$, $D = K/\kappa$, and G^* is the normal derivative of G. The boundary and domain integrals in Eq. 10 are implemented in the Green element sense over elements as in Formulation 1. The unknown quantities are linearly interpolated in time and space so that Eq. 10 for each element Ω^e yields

$$
E_{ij}^m T_j^m + C_{ij}^m q_j^m + U_{ij}T_j^1 + V_i^m Q^m = 0
\tag{12}
$$

where

$$
\begin{aligned}
E_{ij}^m &= D\int_{t_1}^{t_2}v^m(\tau)\int_{\Gamma^e}\varphi_j(r)G^*(r,r_i,t,\tau)\,dsd\tau + 2\delta_{ij}\lambda; \\
C_{ij}^m &= \frac{1}{\kappa}\int_{t_1}^{t_2}v^m(\tau)\int_{\Gamma^e}\varphi_j(r)G(r,r_i,t,\tau)\,dsd\tau; \\
U_{ij} &= \iint_{\Omega^e}\varphi_j(r)G(r,r_i,\Delta t,0)\,dA; \quad V_i^m = \frac{1}{\kappa}\int_{t_1}^{t_2}v^m\iint_{\Omega^e}G(r,r_i,t,\tau)\,dAd\tau
\end{aligned}
\tag{13}
$$

The index $m \in [1,2]$ represents the time levels of the previous and current times t_1 and t_2, v and φ are respectively the interpolating functions in time and space. The expression given by Eq. 12 represents one time-marching scheme that can be employed in implementing this formulation. With this time-marching scheme, the boundary and domain integrations are evaluated at each time step. The other scheme requires that the time integration always restarts at the initial time t_0 [Brebbia et al. (1984)]. Both time marching schemes are coded in the computer program of this formulation. The discrete element equations represented by Eq. 12 are aggregated for all the elements that are employed in discretizing the computational

domain, resulting in a matrix equation that is similar to Eq. 8 with the coefficient matrix, **A**, and unknown vector, **p**, defined as

$$
\mathbf{A} = \begin{bmatrix} E_{ij}^2 \\ C_{ij}^2 \\ V_i^2 \end{bmatrix} \quad \text{and} \quad \mathbf{p} = \begin{Bmatrix} T_j^2 \\ q_j^2 \\ Q^2 \end{Bmatrix} \tag{14}
$$

4 Least square and Tikhonov regularization

Eq (8) is over-determined and its solution is amenable to the least square method, while the matrix **A** is usually ill-conditioned and it is regularized by the Tikhonov regularization method. The decomposition of **A** is facilitated by the singular value decomposition (SVD) method [Golub and Van Loan (1996)].

$$
\mathbf{A} = \mathbf{UDV}^t = \sum_{i=1}^{N} \psi_i u_i v_i^{tr} \tag{15}
$$

where **U** and **V** are, respectively, $M \times M$ and $N \times N$ orthogonal matrices and **D** is an $M \times N$ diagonal matrix with N non-negative diagonal elements ψ_1, ψ_2, ..., ψ_N. The least square solution of Eq. 8 minimises the Euclidian norm $\|\mathbf{Ap} - \mathbf{b}\|^2$, resulting in the solution for the unknowns **p**

$$
\mathbf{p} = \mathbf{B}^{-1}\mathbf{s} = \sum_{i=1}^{N} \frac{u_i^{tr}\mathbf{b}}{\psi_i} v_i \tag{16}
$$

Where $\mathbf{B}=\mathbf{A}^{tr}\mathbf{A}$, $\mathbf{s}=\mathbf{A}^{tr}\mathbf{b}$, and u_i and v_i are the ith column of the matrices **U** and **V**, respectively. The small singular values ψ_i cause instability of the solution for **p**, and this is overcome by using the Tikhonov regularization method which minimizes $\|\mathbf{Ap} - \mathbf{b}\|^2 + \alpha^2 \|\mathbf{Ip}\|^2$ in calculating the solution for **p** [Hansen (1994)]

$$
\mathbf{p}(\alpha) = \sum_{i=1}^{N} \frac{\psi_i}{\alpha^2 + \psi_i^2} u_i^{tr}\mathbf{b}v_i \tag{17}
$$

where α is the regulation parameter whose choice is carefully made so that it is not too small to retain the instability of the numerical solution or too large to have smooth unrealistic results.

5 Numerical Examples

Five numerical examples of transient IHCPs are solved by the two GEM formulations. The first two address the recovery of T and q, while the remaining three address the recovery of the heat source strength Q. The first two examples had been solved by Lesnic et al. (1996), while the others had been addressed by Yan et al. (2008) using the method of fundamental solutions (MFS).

5.1 Example 1

This is a transient example in one spatial dimension. It is solved by the GEM formulations in a 2-D rectangular domain with insulated boundaries at the top and bottom. With the test function $T(x,t)=2t+x^2$ that satisfies the governing Eq. 1 in $x \in [0,1]$, $K=1$, $c=1$ and $Q=0$ and the temperature distribution $T(x,0)=x^2$ is prescribed at the initial time $t=0$. Along the boundary $x=1$, the temperature and flux are specified, that is $T(1,t)+q(1,t)=2t+3$. The boundary along $x=0$ is a Γ_4 boundary where neither T nor q is specified, and three locations with available temperature measurements are examined: (i) $x_m=1$, (ii) $x_m=0.5$ and (iii) $x_m=0.25$. The GEM simulations of this example used only four rectangular elements and a time step, $\Delta t=0.025$, while the values of the regularization parameter for both formulations for the five examples are presented in Table 1. The numerical results from the two GEM formulations are presented in Fig. 2a in terms of the relative error, calculated by Eq. 18 for $T(x,t)$, and as well as in Fig. 2b for $q(x=0,t)$ along the Γ_4 boundary for the three cases. The solutions of Formulation 1 have consistently lower relative error than those of Formulation 2, indicating that Formulation 1 gives better prediction of the temperature and heat flux.

$$\varepsilon = \frac{1}{M} \sqrt{\frac{\sum\limits_{i=1}^{M}(T_i^{cal}-T_i^{exact})^2}{\sum\limits_{i=1}^{M}(T_i^{exact})^2}} \tag{18}$$

5.2 Example 2

This is a transient IHCP with a more stiff test function that is prescribed in $x \in [0,1]$, and it is expressed as [Lesnic et al. (1996); Carslaw and Jaeger (1959)]

$$T(x,t) = \begin{cases} u(x,t), & t \in [0,0.5) \\ u(x,t)-2u(x,t-0.5), & t \in [0.5,1) \\ u(x,t)-2u(x,t-0.5)+2u(x,t-1), & t \in [1,1.5) \\ u(x,t)-2u(x,t-0.5)+2u(x,t-1)-2u(x,t-1.5), & t \in [1.5,2] \end{cases} \tag{19}$$

where

$$u(x,t) = \frac{3(1-x)^2-1}{6} + t - 2\sum_{n=1}^{\infty}\frac{(-1)^n}{n^2\pi^2}\cos[n\pi(1-x)]e^{-n^2\pi^2 t} \tag{20}$$

Along the boundary $x=1$, T and q are specified with $T(1,t)$ obtained from Eq. 19 and $q(1,t)=0$. Measurements of T are available at $x_m=0.25$, while the boundary
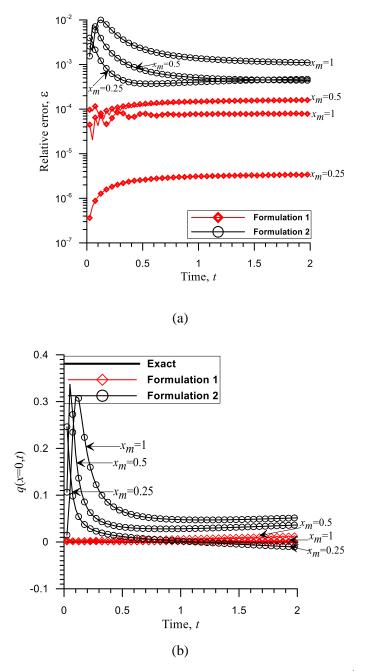
(a)

(b)

Figure 2: GEM simulation results of Example 1: (a) relative error of $T(x,t)$ and (b) $q(x=0,t)$.

Table 1: Values of the regularization parameter, α, used in the simulations of the five examples.

Examples and cases	α	
	Formulation 1	Formulation 2
1 (i)	2.2×10^{-4}	3×10^{-3}
1 (ii)	3×10^{-3}	10^{-2}
1 (iii)	7.1×10^{-4}	1.5×10^{-2}
2	3.2×10^{-4}	5×10^{-2}
3: $\sigma = 0\%$	2.2×10^{-4}	10^{-4}
3: $\sigma = 1\%$	3.2×10^{-4}	10^{-4}
3: $\sigma = 3\%$	3.2×10^{-4}	10^{-4}
3: $\sigma = 5\%$	3.2×10^{-4}	10^{-4}
4: $\sigma = 0\%$	2.2×10^{-4}	10^{-6}
4: $\sigma = 1\%$	3.2×10^{-4}	10^{-6}
4: $\sigma = 3\%$	3.2×10^{-4}	10^{-6}
4: $\sigma = 5\%$	3.2×10^{-4}	10^{-6}
5: $\sigma = 0\%$	2.2×10^{-4}	8×10^{-3}
5: $\sigma = 1\%$	3.2×10^{-4}	8×10^{-3}
5: $\sigma = 3\%$	3.2×10^{-4}	8×10^{-3}
5: $\sigma = 5\%$	3.2×10^{-4}	8×10^{-3}

along $x=0$ is a Γ_4 boundary where neither T nor q is known. Using only 4 rectangular elements, the GEM simulations are carried in a 2-D domain with a uniform time step $\Delta t=0.025$. The temporal variation of the relative error ε for the spatial temperature distribution, and the flux at $x=0$ for the two GEM formulations are respectively presented in Figs. 3 and 4. As with the first example, the relative error of the solution for the temperature from Formulation 1 is lower than that from Formulation 2, and Formulation 1 gives better prediction of the flux at $x=0$.

5.3   *Example 3*

In this example, the recovery of the strength of the heat source is sought. The exact solution to Eq. 1 in 1-D spatial domain $x \in [0,1]$ that is used as the test function is

$$T(x,t) = \frac{x^4}{4} + 3tx^2 + \sin(x)e^{-t} \qquad (21)$$

It gives an expression for the heat source, $Q(t) = -6t$. Dirichlet boundary conditions are specified along $x=0$ and $x=1$, while temperature measurements are available
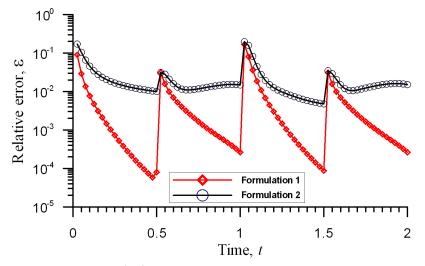
Figure 3: Error plots of $T(x,t)$ with time from the two GEM formulations for Example 2.
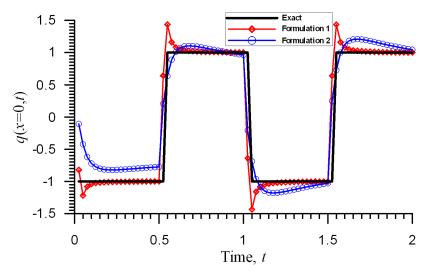

Figure 4: GEM simulations of the variation of the flux at $x=0$ with time for Example 2.

at x_m=0.5 for all times. The GEM simulations are implemented in a rectangular domain that is discretized with 10 linear rectangular elements. A uniform time step of 0.025, and the temperature data at x=0, 0.5 and 1 are perturbed randomly with noise levels of σ=1, 3 and 5%. The values of the regularization parameters used in both formulations are found in Table 1. The numerical results from both GEM formulations for the heat source are presented in Fig. 5 for various noise levels. The results from both formulations when there is no noise in the data are left out of Fig. 5 because they correctly reproduced the exact solution. The plots of the relative error, ε, from both formulations are presented in Fig. 6. Formulation 2 produced more accurate and stable solutions than Formulation 1 for the various noise levels.
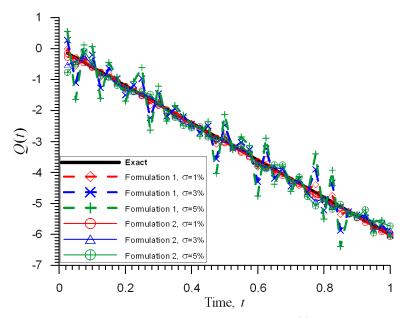

Figure 5: GEM simulations for the heat source $Q(t)$ of Example 3.

5.4 Example 4

In this example, the test function that satisfies Eq. 1 in $x \in [0, 1]$ is

$$T(x,t) = x^2 + 2t + \sin(2\pi t) \tag{22}$$

The corresponding expression for the heat source is $Q(t) = 2\pi\cos(2\pi t)$. Along x=0 and x=1 the temperature is specified, and its measurements are available at x_m=0.5 for all times. The GEM simulations use 10 linear rectangular elements, a uniform
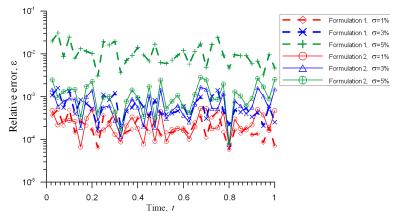
Figure 6: Error plots of $T(x,t)$ with time from the two GEM formulations for Example 3.

time step Δt=0.025, and the temperature data at x=0, 0.5 and 1 are perturbed randomly with noise levels of σ=1, 3 and 5%. The GEM and exact solutions for the heat source are presented in Fig. 7 for various noise levels. Though not shown in Fig. 7, the numerical results from the two GEM formulations reproduced the exact solution when there is no noise in the data. The values of the regularization parameter used in the two formulations are found in Table 1. The plots of the relative error, ε, from the two formulations are presented in Fig. 8. The results from Formulation 2 are slightly more accurate than those of Formulation 1, but they are oscillatory for both formulations at noise levels of 3% and 5%.

5.5 Example 5

In this example, also previously simulated by Yan et al. (2008) using the MFS, the IHCP is governed by Eq. 1 in a 1-D homogeneous domain $x \in [0,1]$. Dirichlet conditions with zero temperature are specified along x=0 and x=1. Initially the temperature is zero everywhere in the domain, and the IHCP problem is to recover the step-wise heat source distribution expressed as:

$$Q(t) = \begin{cases} -1, & t \in (0, 0.25) \\ 1, & t \in [0.25, 0.5) \\ -1, & t \in [0.5, 0.75) \\ 1, & t \in [0.75, 1] \end{cases} \tag{23}$$

In the absence of an analytic solution, the temperature distribution is generated by solving the direct problem with GEM using fine spatial and temporal discretizations
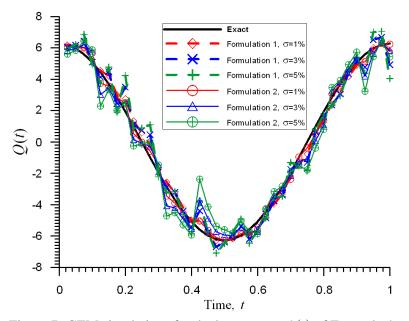
Figure 7: GEM simulations for the heat source $Q(t)$ of Example 4.
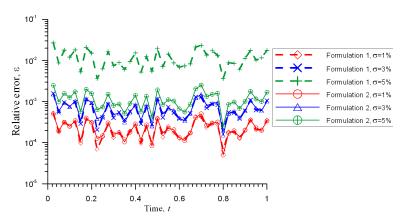

Figure 8: Error plots of $T(x,t)$ with time from the two GEM formulations for Example 4.

of 40 linear rectangular elements and time step $\Delta t = 2.5 \times 10^{-3}$. The generated direct GEM solution is presented in Figure 9. The inverse modeling with GEM is carried out in a 2-D rectangular domain using the specified boundary conditions: $T(x=0,t) = T(x=1,t) = 0$, the initial condition: $T(x,0) = 0$, and the temperature data at $x_m=0.5$ that were generated by the direct GEM.
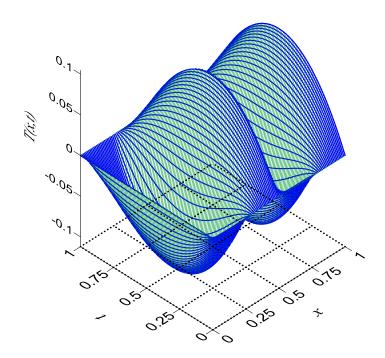

Figure 9: Direct GEM solution of the temperature for Example 5.

Ten linear rectangular elements are used in the inverse GEM simulations with no-heat flux boundaries imposed on the top and bottom boundaries. A uniform time step $\Delta t=0.025$ is used in both GEM formulations. Because of the homogeneous boundary conditions, only the temperature data at $x=0.5$ are affected when they are randomly perturbed with noise levels $\sigma=1$, 3 and 5%. The values of the regularization parameter employed in the GEM simulations are found in Table 1. To eliminate clutter of the results, only the solution of zero and 5% noise levels are presented. The simulated results from the two formulations for the heat source strength are presented in Fig. 10, while the plots of relative error, ε, for the temperature are presented in Fig. 11. The GEM Formulation 1 solutions for the temporal variation of the heat source and the temperature are superior to those of Formulation 2. The

solutions from both formulations are superior to those obtained by Yan et al. (2008) who used the method of fundamental solutions.
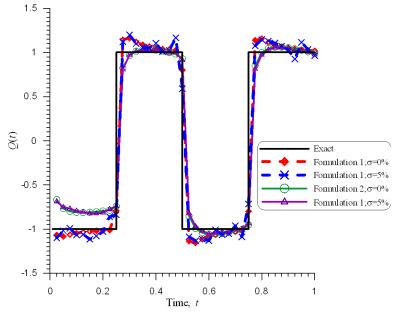

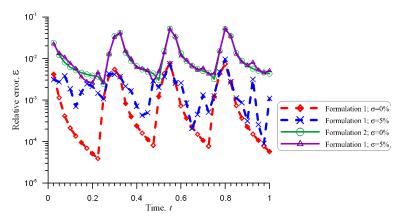Figure 10: Heat source recovery of Example 5.

Figure 11: Error plots of $T(x,t)$ with time from the two GEM formulations for Example 5.

6   Conclusion

Two Green element formulations, which are based on the singular integral theory of BEM, have been used to solve transient IHCPs in 2-D homogeneous domains. Both formulations produced over-determined and ill-condition systems of discrete equations which are solved by the least square method with Tikhonov regularization. With both formulations applied to five numerical examples, Formulation 1, which uses the fundamental solution of the Laplace operator, generally gives more accurate results than Formulation 2, which uses the fundamental solution of transient diffusion equation. Although this result may run contrary to the intuitive reason that Formulation 2 should produce more accurate results than Formulation 1 since it uses the fundamental solution of the heat conduction equation, however the numerical errors from manipulating its complicated fundamental solution compromise the quality of its results. This also influences the computing speed of Formulation 2 which is about 30 times slower than Formulation 1.

References

Brebbia, C. A.; Telles, J. C. F.; Wrobel, L. C. (1984): *Boundary Element Techniques*, Springer-Verlag, NY.

Carslaw, H. S.; Jaeger, J. C. (1959): *Conduction of Heat in Solids*, Oxford Univ. Press, UK.

Char, M-I.; Chang, F-P.; Tai, B-C. (2008): Inverse determination of thermal conductivity by differential quadrature method, *Int. Comm. Heat Mass Trans.*, vol. 35, pp. 113-119.

Cialkowski, M. J.; Grysa, K. (2010): A sequential and global method of solving an inverse problem of heat conduction equation. *J. Theo. and App. Mech.*, vol. 48, pp. 111-134.

Golub, G. H.; Van Loan, V. F. (1996): *Matrix Computations*, John Hopkins Univ. Press, Baltimore, USA.

Hansen, P. C. (1994): Regularization Tools: a Matlab Package for Analysis and Solution of Discrete Ill-posed Problems. *Numer. Algorithms*, vol. 6, pp. 1-35.

Lesnic, D.; Elliot, L.; Ingham, D. B. (1996): Application of the boundary element method to inverse heat conduction problems. *Int. J. Heat Mass Trans.*, vol. 39 pp. 1503-1517.

Masood, K.; Messaoudi, S.; Zaman, F. D. (2002): Initial inverse problem in heat equation with Bessel operator. *Int. J. Heat Mass Trans.*, vol. 45, pp. 2959-2965.

Mera, N. S.; Elliott, L.; Ingham, D. B. (2004):Numerical solution of a boundary detection problem using genetic algorithms. *Engrg. Anal. Bound. Elem.*, vol. 28,

pp. 405–411.

Mierzwiczak, M.; Kolodziej, J. A. (2010): Application of the method of fundamental solutions and radial basis functions for inverse transient heat source problem. *Comp. Phy. Comm.*, vol. 181, pp. 2035-2043.

Pereverzyev, S. S.; Pinnau, R.; Siedow, N. (2005): Initial temperature reconstruction for nonlinear heat equation: application to a coupled radiative-conductive heat transfer problem. *Inv. Prob. Sc. Engrg.*, vol. 16, pp. 55-67.

Popov, V.; Power, H.; Skerget, L. (Eds.) (2007): *Domain Decomposition Techniques for Boundary Elements: Application to Fluid Flow*, Wit Press, Southampton, UK.

Reinhardt, H. J.; Hao, D. N.; Frohne, J.; Suttmeier, F. T. (2007): Numerical solution of inverse heat conduction problems in two spatial dimensions. *J. Inverse and Ill-posed Prob.*, vol. 15, pp. 181-198.

Sawaf, B.; Özisik, M. N.; Jarny, Y. (1995): An inverse analysis to estimate linearly temperature dependent thermal conductivity components and heat capacity of an orthotropic medium. *Int. J. Heat Mass Trans.*, vol. 38, pp. 3005-3010.

Sladek, J.; Sladek, V.; Hon, Y. C. (2006): Inverse heat conduction problems by meshless local Petrov–Galerkin method. *Engrg. Anal. Bound. Elem.*, vol. 30, pp. 650-661.

Taigbenu, A. E. (1999): *The Green Element Method*, Kluwer, Boston, USA (1999).

Taigbenu, A. E. (2012): Enhancement of the accuracy of the Green element method: Application to potential problems. *Engrg. Anal. Bound. Elem.*, vol. 35, pp. 125-136.

Taigbenu, A. E. (2015): Inverse solutions of temperature, heat flux and heat source by the Green element method. *Appl. Math. Modell.*, vol. 39, pp. 667-681.

Wei, T.; Wang, J. C. (2012): Simultaneous determination for a space-dependent heat source and the initial data by the MFS. *Engrg. Anal. Bound. Elem.*, vol. 36, pp. 1848–1855.

Wei, T.; Wang, J. C. (2012): Simultaneous determination for a space-dependent heat source and the initial data by the MFS. *Engrg. Anal. Bound. Elem.*, vol. 36, pp. 1848-1855.

Yan, L.; Fu, C-L.; Yang, F-L. (2008): The method of fundamental solutions for the inverse heat source problem. *Engrg. Anal. Bound. Elem.*, vol. 32, pp. 216-222.

Yang, C. (1998): A linear inverse model for the temperature-dependent thermal conductivity determination in one-dimensional problems. *App. Math. Mod.*, vol. 22, pp. 1-9.

Yang, F.; Yan, L.; Wei, T. (2009): Reconstruction of the corrosion boundary for the Laplace equation by using a boundary collocation method. *Math. Comp. Sim.*, vol. 79, pp. 2148-2156.